Materials Research Bulletin 45 (2010) 1875–1882

Contents lists available at ScienceDirect

Materials Research Bulletin

journal homepage: www.elsevier.com/locate/matresbu

Phase stability study of $Bi_{0.15}Sr_{0.85-x}Ae_xCoO_{3-\delta}$ (x = 0 and $Ae = Ba_{0.28}$; $Ca_{0.17}$) perovskites by in-situ neutron diffraction

A.K. Eriksson [a,1], S.G. Eriksson [a], L.C. Chapon [b], C.S. Knee [c,*]

[a] Department of Environmental Inorganic Chemistry, Chalmers University of Technology, SE-412 96 Göteborg, Sweden
[b] STFC, Rutherford Appleton Lab, ISIS Facility, Didcot OX11 0 QX, Oxon, England
[c] Department of Chemistry, University of Gothenburg, SE-412 96 Göteborg, Sweden

ARTICLE INFO

Article history:
Received 28 May 2010
Received in revised form 26 August 2010
Accepted 2 September 2010
Available online 15 September 2010

Keywords:
Oxides
Neutron scattering
Phase transitions
Ionic conductor
TGA

ABSTRACT

The oxygen deficient perovskites, $Bi_{0.15}Sr_{0.85-x}Ae_xCoO_{3-\delta}$, x = 0 and $Ae_x = Ba_{0.28}$, $Ca_{0.17}$, were studied with in-situ neutron powder diffraction and combined TGA/DSC in order to investigate their behaviour at elevated temperatures in oxidising conditions. The phase stability of the $I4/mmm$ supercell structure adopted by $Bi_{0.15}Sr_{0.85}CoO_{3-\delta}$ is shown to be dependent on temperature and the oxygen content of the phase, with three structural events, at T ~ 250, 590 and 880 °C, detected. The first transition occurs as the perovskite supercell vanishes due to oxygen absorption; the second transition is also associated with oxidation and involves the decomposition of the perovskite phase via an exothermic process to yield a dominant hexagonal phase. Finally, at T ~ 900 °C the perovskite phase re-forms. For the Ba and Ca containing materials the decomposition to the hexagonal phase occurs at T ~ 600 °C and ~ 650 °C respectively. The presence of Ca at the A-site is found to stabilise the $I4/mmm$ supercell structure in the range RT - 650 °C. The antiferromagnetic to paramagnetic transitions occur at $T_N \sim 250$ °C, $T_N \sim 175$ °C and $T_N \sim 145$ °C for the samples with $Ae_x = Ba_{0.28}$, x = 0 and $Ae_x = Ca_{0.17}$, respectively.

1. Introduction

The perovskite compounds $BiCoO_3$ and $SrCoO_3$ are unstable at elevated temperatures, and the former can only be obtained at high pressures [1]. However, the oxygen deficient brownmillierite phase $SrCoO_{2.5}$ can be obtained by quenching from high temperature (T > 900 °C) [2]. Alternatively, synthesis at lower temperatures, combined with slow furnace cooling, leads to the formation of a cobalt deficient phase $Sr_6Co_5O_{15}$ with a rhombohedral structure in air [3] or nitrogen [4] atmospheres. Upon replacing more than 20% of Sr^{2+} by a lanthanide ion, Ln^{3+}, the perovskite $Ln_{1-y}Sr_yCoO_{3-\delta}$ solid solutions have been proven to be stable and can readily be synthesised in air [5]. The oxygen deficiency in these materials creates pathways for oxide ion migration and this, coupled to mixed cobalt valence states, makes them suitable as mixed electronic and ionic conductors (MIEC) electrodes in solid oxide fuel cells (SOFCs) or as oxygen permeable membranes [6–8]. The magnetic properties also show a wide range of responses depending on the amount of dopant and the oxygen content. Behaviour spanning from room temperature ferromagnetism, [9] spin glass, [10] and long range G-type antiferromagnetic ordering have been reported [11].

In 2003 a new form of oxygen defect based perovskite superstructure was reported for $Sr_{0.33}Ln_{0.67}CoO_{3-\delta}$ Ln = Y, Ho and Dy, [12] and $Y_{0.3}Sr_{0.7}CoO_{2.62}$ [13] phases. In contrast to the brownmillerite structure, in which the oxygen deficient layers form chains of CoO_4 tetrahedra running along the [110] direction, segregated Co_4O_{12} units are found in these materials and the structure is described using a tetragonal, $I4/mmm$, supercell with $a \approx 2a_p$, $c \approx 4a_p$. Structural analysis of the $Ln_{1-y}Sr_yCoO_{3-\delta}$ phases, [14] ($Ln = Sm^{3+} \rightarrow Yb^{3+}$, $x = 0.67 \geq x \geq 0.9$) revealed that the extent of cation ordering at the A-site, and the linked tendency for supercell formation, is correlated to the size of the rare earth ion. Thus, earlier rare earth elements adopt a simple cubic cell ($Pm\bar{3}m$, $a = a_p$) with cations disordered on a single A-site.

Compositions similar to the $Ln_{1-y}Sr_yCoO_{3-\delta}$ phase with Ln^{3+} replaced by Bi^{3+} have previously been studied. The Bi^{3+} ion exhibits an intermediate ionic size to the Y^{3+} and La^{3+} ions, and it was reported by Tolochko et al. [15] that $Bi_{1-y}Sr_yCoO_{3-\delta}$ with y = 0.8 and 0.9 form cubic phases when quenched. Knee et al. [16] studied the same materials, i.e., $Sr_{1-y}Bi_yCoO_{3-\delta}$ ($0.1 \leq y \leq 0.2$) and found additional supercell reflections consistent with the $I4/mmm$ superstructure in quenched, as-prepared, samples. Similar TG/DSC plots were given in both reports, with a mass gain in the T interval 300-500 °C and exothermic peaks at 650-720 °C with associated mass gains. It was proposed by Knee et al. [16] that the

---

[*] Corresponding author.
E-mail address: knee@chem.gu.se (C.S. Knee).
[1] Present address: Department of Materials Science and Engineering, NTNU, NO-7491 Trondheim, Norway.

0025-5408/$ – see front matter © 2010 Elsevier Ltd. All rights reserved.
doi:10.1016/j.materresbull.2010.09.004

exotherms observed at 660 °C and 710 °C for the y = 0.10 and 0.20 $Sr_{1-y}Bi_yCoO_{3-\delta}$ samples respectively were attributable to a structural phase transition from the tetragonal supercell to a cubic ($Pm\bar{3}m$) perovskite structure. In recently published work documenting the effects of cationic substitution of $Bi_{0.15}Sr_{0.85-x}Ae_xCoO_{3-\delta}$ perovskites, where $Ae_x = Ca_{0.17}$ or $Ba_{0.28}$, it was found that the ionic size of the A-site dopant affects both the structure, magnetic properties and the oxygen absorption/de-sorption behaviour [17]. In this work we have investigated the different phase transitions using in-situ neutron diffraction and TG/DSC to clarify the thermal phase stability of the $Bi_{0.15}Sr_{0.85-x}Ae_xCoO_{3-\delta}$ materials.

2. Experimental

The sample preparation of $Bi_{0.15}Sr_{0.85-x}Ae_xCoO_{3-\delta}$ (x = 0 and $Ae_x = Ba_{0.28}$, $Ca_{0.17}$) was performed via the solid state method. Stoichiometric quantities of high purity $SrCO_3$, $BaCO_3$ or $CaCO_3$, Bi_2O_3, and CoO powders were mixed using an agate mortar and pestle and then heated at 800 °C for 20 h. The reactants were then pressed into pellets and fired at 850, 900 and 925 °C for similar lengths of time overnight with intermediate regrinding to obtain a homogenous phase. The samples were quenched to room temperature (RT) in air by placing the alumina crucibles onto a metallic plate after every heat treatment.

Phase purity was determined using a Siemens D5000 powder x-ray diffractometer with an energy dispersive Sol-X^{TM} detector and Neutron powder diffraction (NPD) data collected in the 2θ range 15–60°. Neutron diffraction measurements as a function of temperature were carried out on the GEM instrument at the ISIS facility, Rutherford Appleton Laboratories, Chilton, UK. Initially a RT scan was measured for 1 h, to establish a correction file from the empty silica sample tube and furnace. A silica tube designed to withstand thermal expansion and different gas pressures was filled with approx. 5.5 g of sample. The temperature was measured by two thermocouples placed close to the sample but above the incoming neutron beam. The silica sample holder was placed in the furnace and the sample exposed to a neutron beam of 4 cm height. The sample was kept under a constant pressure of oxygen (~ 785 mbar) and the pressure was monitored via a Nernstian sensor (Systech Instruments, Oxford, U.K.). The first sample scan was measured at RT and then the furnace was slowly heated to 100 °C, where the second scan started after reaching thermal equilibrium. A heating ramp of 1°/min was established with scans collected every 5 min on heating to 800 °C, at which point a 1 h scan was measured (this long scan was taken at 740 °C for $Bi_{0.15}Sr_{0.57}Ba_{0.28}CoO_{3-\delta}$). Thereafter on cooling to 300 °C a final scan was taken. Data was collected on detector banks 1 to 6, covering an approximate *d*-spacing range of 0.5–20 Å. Analysis of the nuclear and magnetic structures proceeded using the Rietveld refinement program GSAS, [18] and data from banks 3 (*d*-range = 0.54–2.70 Å), 4 (*d*-range = 0.74–4.1 Å) and 5 (*d*-range = 1.30–7.15 Å). The SeqGSAS routine was used to analyse the ramping data and refine the cell parameter and oxygen content for all samples using a cubic ($Pm\bar{3}m$) structural model. Nine variables including lattice constant, background and peak profile parameters, and the occupancy factor for the 3*d* (0,0,0.5) oxygen site were refined.

To monitor the oxygen uptake and phase stability of the $Bi_{0.15}Sr_{0.85-x}Ae_{-x}CoO_{3-\delta}$ samples, thermal analysis was performed in a simultaneous thermogravimetric (TG)–differential scanning calorimeter (DSC) NETZSCH STA 409 PC Luxx thermal analyser. The samples were placed in an alumina crucible and heated from RT to 950 °C with a heating rate of 5° C/min, and then kept at 950 °C for 30 min before cooling to RT at 5 °C/min. The atmosphere used was a mixture of synthetic air and nitrogen with individual gas flow rates of 10 ml/min.

3. Results

3.1. Structural analysis

The Rietveld fit to the RT data collected on detector bank 4 from the $Bi_{0.15}Sr_{0.85}CoO_{3-\delta}$ sample is shown in Fig. 1a. The RT structure determined from constant wavelength neutron data was reported previously by Knee *et al.* [16] and the data presented here verified those results. In particular the reflections found in detector bank 2 at $d \approx 7.8$ Å and bank 4 $d \approx 2.55$ Å, confirmed the supercell ($I4/mmm$) structure with cell parameters $a = 7.788(4)$ Å and $c = 15.576(2)$ Å. The RT data of $Bi_{0.15}Sr_{0.85-x}Ae_xCoO_{3-\delta}$, $Ae = Ba_{0.28}$ and $Ca_{0.17}$, also displayed similar results as our previous report on the same compounds, [17] with cubic ($Pm\bar{3}m$, $a = 3.914(1)$ Å) and supercell ($I4/mmm$, $a = 7.730(1)$ and $c = 15.504(4)$ Å) structures, respectively. Further details of the structural parameters determined at RT are given in Table 1.

The RT phases exhibited antiferromagnetic long range order, which was modelled with a G-type antiferromagnetic model to give an ordered magnetic moment of 1.76(1) μ_B for $Bi_{0.15}Sr_{0.85}CoO_{3-\delta}$. The Néel temperature of ~ 175 °C was determined based on the decay of the most intense magnetic reflection at $d \sim 4.5$ Å in bank 3 which can be seen in Fig. 2a. In the figure we also observe how the $I4/mmm$ supercell reflections remain up to $T > 200$ °C, but slowly decay and vanish at $T \sim 250$ °C, above which the structure reverts to a primitive cubic cell as oxygen vacancy ordering is lost. The Rietveld fit to the 300 °C data set based on a $Pm\bar{3}m$ model is shown in Fig. 1b. In contrast to $Bi_{0.15}Sr_{0.85}CoO_{3-\delta}$, the supercell

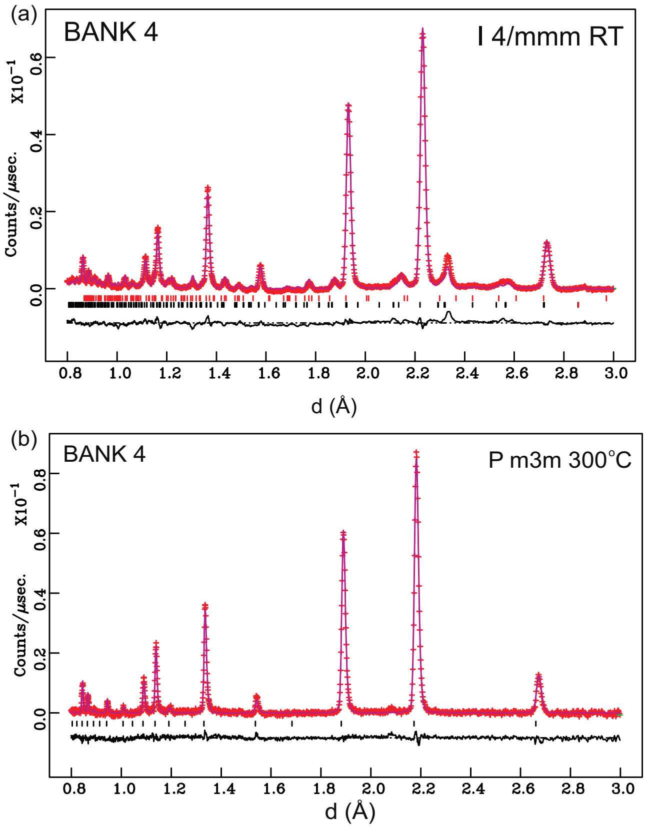

Fig. 1. The Rietveld fit achieved to data collected on GEM for $Bi_{0.15}Sr_{0.85}CoO_{3-\delta}$ at (a) RT and (b) 300 °C. Crosses are observed data points, upper line is the calculated profile and lower line is the difference between observed and calculated intensities. The RT pattern exhibits a supercell ($I4/mmm$) and the 300 °C pattern is modelled with a cubic unit cell ($Pm\bar{3}m$). Magnetic scattering is fitted via a second phase (upper tick marks) in the RT analysis.